Med Chem Res
DOI 10.1007/s00044-015-1367-z

MEDICINAL CHEMISTRY RESEARCH

ORIGINAL RESEARCH

Inhibition of Alzheimer's BACE-1 by 2,6-dialkyl-4-chromon-3-yl-1,4-dihydropyridine-3,5-dicarboxylates

Nima Razzaghi-Asl[1,2] · Neha Aggarwal[3] · Smriti Srivastava[3] · Virinder S. Parmar[3] · Ashok K. Prasad[3] · Ramin Miri[4] · Luciano Saso[5] · Omidreza Firuzi[4]

Received: 14 September 2014 / Accepted: 9 April 2015

Abstract Alzheimer's disease is the most common cause of dementia in the elderly, and no disease-modifying therapy is yet available for this devastating pathology. Deposition of different physicochemical forms of amyloid-β peptides is a critical phase in the pathogenesis of Alzheimer's disease. β-Site amyloid precursor protein cleaving enzyme 1 (BACE-1) is a major enzyme responsible for amyloid-β production; therefore, inhibition of this enzyme represents a promising approach for the discovery of amyloid-β-lowering agents. In this study, a series of novel 2,6-dialkyl-4-chromon-3-yl-1,4-dihydropyridine-3,5-dicarboxylates (**14**–**23**) were synthesized and assessed as BACE-1 inhibitors using the Förster resonance energy transfer-based enzyme assay. Synthesized dihydropyridines exhibited weak-to-relatively-good BACE-1 inhibitory activities. Enzyme inhibitory activities ranged from 6.84 ± 6.62 (**23**) to 51.32 ± 1.04 (**14**) percent enzyme inhibitions at the concentration of 10 μM. The structure–activity relationship study showed that the presence of 4-[7-(ethanoyloxy)-4-oxo-4H-chromen-3-yl] moiety at C4 position of dihydropyridine ring (**14**, **16** and **18**) confers higher activity compared with other substitutions at this position. Docking simulation predicted a key H-bond interaction between Asp32 residue and dihydropyridine NH group. Moreover, all docked dihydropyridines made good hydrophobic contacts with S1 and S2 subpockets of BACE-1. A good correlation between estimated binding affinities (pK_i) and experimental BACE-1 inhibitory activities at 10 μM was obtained ($R^2 = 0.639$). The findings of this study suggested that 2,6-dialkyl-4-chromon-3-yl-1,4-dihydropyridine-3,5-dicarboxylates could be promising scaffolds for the discovery of novel BACE-1 inhibitors for management of Alzheimer's disease.

Keywords Alzheimer · BACE-1 · Dihydropyridine · Inhibitor

Electronic supplementary material The online version of this article (doi:10.1007/s00044-015-1367-z) contains supplementary material, which is available to authorized users.

✉ Omidreza Firuzi
foomid@yahoo.com;
firuzio@sums.ac.ir

[1] Department of Medicinal Chemistry, School of Pharmacy, Ardabil University of Medical Sciences, Ardabil, Iran

[2] Drug and Advanced Sciences Research Center, School of Pharmacy, Ardabil University of Medical Sciences, Ardabil, Iran

[3] Bioorganic Laboratory, Department of Chemistry, University of Delhi, Delhi, 110 007, India

[4] Medicinal and Natural Products Chemistry Research Center, Shiraz University of Medical Sciences, 71348-53734 Shiraz, Iran

[5] Department of Physiology and Pharmacology "Vittorio Erspamer", Sapienza University of Rome, P. le Aldo Moro 5, 00185 Rome, Italy

Introduction

Alzheimer's disease (AD) is a neurodegenerative disorder characterized by a progressive decline in memory and other cognitive functions and is the main cause of dementia in the elderly (McKhann *et al.*, 1984; Verdon *et al.*, 2007; Reitz *et al.*, 2011). The main neuropathological hallmarks of AD are the presence of extracellular amyloid-β (Aβ) plaques and intracellular neurofibrillary tangles in the brain. Accumulation of different physicochemical forms of Aβ peptides in the extracellular space of the brain is believed to begin the neurodegeneration in patients afflicted with AD (Selkoe, 2008). Proteolytic cleavage of the large transmembrane amyloid-β precursor protein (APP) by the

Published online: 05 May 2015

consecutive actions of β-secretase and γ-secretase enzymes results in the production of Aβ peptides (Vassar, 2002).

β-Secretase (β-site APP cleaving enzyme 1 or BACE-1) is a type I membrane-associated aspartyl protease and is the rate-limiting enzyme in Aβ production. BACE-1 is an attractive target for the discovery of disease-modifying therapies in AD (Sinha *et al.*, 1999). Final generation of Aβ peptides is carried out by subsequent cleavage of APP by γ-secretase; however, inhibition of this enzyme may be associated with some mechanism-based adverse effects (John *et al.*, 2003).

Previous studies have demonstrated that BACE-1 knockout mice have negligible Aβ production (Bassil and Grossberg, 2009), and several research groups have generated various BACE-1 inhibitors (Silvestri, 2009; Ghosh *et al.*, 2012) that have lowered Aβ production in vitro and in vivo (Lahiri *et al.*, 2014).

In the earlier attempts, peptidic BACE-1 inhibitors were designed mimicking the conformation of substrates at transition state (Ghosh *et al.*, 2012), but the major drawback of peptidic BACE-1 inhibitors is related to their poor pharmacokinetic profile, which prevents them from being further developed to oral bioavailable CNS drugs. Thus, recent attempts have been directed towards the discovery of small molecule BACE-1 inhibitors (Silvestri, 2009).

1,4-Dihydropyridine is a privileged structure with a wide range of pharmacological activities (Miri *et al.*, 2008; Kumar *et al.*, 2011). Little attention has been directed towards the BACE-1 blocking activity of these compounds (Choi *et al.*, 2010). Choi and coworkers have reported novel *N*-methylsulfonamide-1,4-dihydropyridine derivatives as BACE-1 inhibitors that exhibited IC_{50} values of 8–30 μM in a cell-based assay (Choi *et al.*, 2010). We have also previously observed that 3,5-bis-*N*-(aryl/heteroaryl) carbamoyl-4-aryl-1,4-dihydropyridines show high potential for inhibition of BACE-1 (Razzaghi-Asl *et al.*, 2013).

In continuation of our interest in the discovery of non-peptidic BACE-1 inhibitors (Razzaghi-Asl *et al.*, 2013; Edraki *et al.*, 2013) and also to further expand the capacity of 1,4-dihydropyridines as privileged small molecule medicinal scaffolds (Chhillar *et al.*, 2006, 2009; Miri *et al.*, 2010, 2012), we herein report the synthesis, assessment of in vitro BACE-1 inhibitory activity and molecular docking study of a series of 2,6-dialkyl-4-chromon-3-yl-1,4-dihydropyridine-3,5-dicarboxylates.

Materials and methods

Chemistry

Chemicals were obtained from Sigma-Aldrich Co. (USA) and SD Fine Ltd., Mumbai, India. AR-grade organic solvents were used without any further purification. Melting points were determined on Buchi M-560 instrument and are uncorrected. The IR spectra are recorded on a PerkinElmer model 2000 FT-IR spectrometer by making KBr disk for solid samples and thin film for oils. The ^{1}H and ^{13}C NMR spectra were recorded on JEOL ALPHA-400 spectrometer at 400 MHz and 100.5 MHz, respectively, using TMS as internal standard. The chemical shift values were on δ scale, and the coupling constants (J) were in Hz. Signals from OH to NH groups in ^{1}H NMR spectra were confirmed by D_2O exchange. HR-ESI-TOF-MS analyses were carried out on a microTOF-Q instrument from Bruker Daltonics, Bremen. Reactions were conducted under an atmosphere of nitrogen when anhydrous solvents were used. Analytical TLCs were performed on pre-coated Merck silica gel $60F_{254}$ plates, and the spots were detected under UV light. Silica gel (100–200 mesh) was used for column chromatography.

General procedure for synthesis of compounds 14–23

The synthesis of compounds **14–23** has been achieved starting from 2,4-dihydroxyacetophenone (**1**) and 2,5-dihydroxyacetophenone (**2**), which were mono-acetylated at C4 or C5 hydroxyl group with acetic anhydride followed by the Vilsmeier–Haack formylation reaction on resultant acetylated compounds **3** and **4** to give 7-acetoxy-3-formylchromone (**5**) and 6-acetoxy-3-formylchromone (**6**), respectively. The chromones **5** and **6** were deacetylated with NaOH to give the corresponding hydroxychromones **7** and **8**. Hantzsch pyridine reaction on 7-hydroxy-3-formylchromone (**7**) and 6-hydroxy-3-formylchromone (**6**) with various β-ketoesters in the presence of catalytic amount of Ba $(NO_3)_2$ yielded the desired hydroxychromonyldihydropyridines **9–13** in 39–42 % overall yields from dihydroxyacetophenones.

Further, the acylation of the chromonyldihydropyridines **9–13** with acetic and hexanoic anhydrides in THF afforded a series of 7-*O*-acetoxychromonyldihydropyridines **14**, **16** and **18**, 7-*O*-hexanoylchromonyldihydropyridines **15**, **17** and **19**, 6-*O*-acetoxychromonyldihydropyridines **20** and **22** and 6-*O*-hexanoylchromonyldihydropyridines **21** and **23** in 70–85 % yields. Characteristic data of synthesized compounds are as follows:

*Dimethyl 4′-(7-hydroxychromon-3-yl)-2′,6′-dimethyl-1′,4′-dihydropyridine-3′,5′-dicarboxylate (**9**)* Compound **9** was obtained as yellow solid in 65 % yield; M.P. 283–285 °C; IR (KBr) ν_{max} 3314, 3244, 1663, 1626, 1599, 1506, 1340, 1223, 1124, 1019, 847 and 781 cm^{-1}, ^{1}H NMR (400 MHz, DMSO): δ 2.20 (6H, s), 3.56 (6H, s), 4.81 (1H, s), 6.76 (1H, *d*, $J = 2.2$ Hz), 6.87 (1H, *dd*, $J = 8.8$ and 2.2 Hz), 7.76 (1H, s), 7.84 (1H, *d*, $J = 8.8$ Hz), 8.32 (1H, s) and

8.92 (1H, s); ^{13}C NMR (100.5 MHz, DMSO): δ 18.12, 32.97, 50.60, 98.00, 101.96, 114.78, 117.02, 125.43, 126.82, 146.56, 153.34, 157.16, 162.15, 167.48 and 174.80; HR-ESI-TOF-MS: *m/z* 408.1041 [M + Na]$^+$, calculated for [$C_{20}H_{19}NO_7$ + Na]$^+$ 408.1054.

*Diethyl 4′-(7-hydroxychromon-3-yl)-2′,6′-dimethyl-1′,4′-dihydropyridine-3′,5′-dicarboxylate (**10**)* Compound **10** was obtained as yellow solid in 63 % yield; M.P. 241–243 °C; IR (KBr) ν_{max} 3619, 3310, 1702, 1678, 1625, 1500, 1306, 1252, 1201, 1095, 848 and 748 cm^{-1}, ^{1}H NMR (400 MHz, DMSO): δ 1.14 (6H, *t*, *J* = 7.3 Hz), 2.20 (6H, s), 3.93–4.08 (4H, m), 4.79 (1H, s), 6.78 (1H, *d*, *J* = 2.2 Hz), 6.87 (1H, *dd*, *J* = 8.8 and 2.2 Hz), 7.78 (1H, s), 7.85 (1H, *d*, *J* = 8.8 Hz), 8.32 (1H, s) and 8.85 (1H, s); ^{13}C NMR (100.5 MHz, DMSO) δ 14.20, 18.27, 33.24, 58.83, 98.22, 101.97, 114.73, 117.11, 125.90, 126.81, 146.43, 153.65, 157.11, 162.08, 166.99 and 174.52; HR-ESI-TOF-MS: *m/z* 436.1356 [M + Na]$^+$, calculated for [$C_{22}H_{23}NO_7$ + Na]$^+$ 436.1367.

*Diethyl 4′-(7-hydroxychromon-3-yl)-2′,6′-dipropyl-1′,4′-dihydropyridine-3′,5′-dicarboxylate (**11**)* Compound **11** was obtained as yellow solid in 62 % yield; M.P. 177–179 °C; IR (KBr) ν_{max} 3619, 3306, 2968, 1702, 1677, 1624, 1499, 1300, 1245, 1198, 1099, 848 and 768 cm^{-1}, ^{1}H NMR (400 MHz, DMSO) δ 0.87 (6H, *t*, *J* = 7.4 Hz), 1.12 (6H, *t*, *J* = 7.3 Hz), 1.43–1.54 (4H, m), 2.39–2.46 (2H, m), 2.66–2.73 (2H, m), 3.92–4.05 (4H, m), 4.81 (1H, s), 6.74 (1H, *d*, *J* = 2.2 Hz), 6.84 (1H, *dd*, *J* = 8.8 and 2.2 Hz), 7.66 (1H, s), 7.82 (1H, *d*, *J* = 8.8 Hz), 8.74 (1H, s) and 10.64 (1H, s); ^{13}C NMR (100.5 MHz, DMSO): δ 13.73, 14.17, 21.88, 32.73, 32.91, 58.90, 98.08, 101.96, 114.72, 117.03, 126.09, 126.87, 150.48, 153.27, 157.11, 162.08, 166.74 and 174.42; HR-ESI-TOF-MS: *m/z* 492.1969 [M + Na]$^+$, calculated for [$C_{26}H_{31}NO_7$ + Na]$^+$ 492.1993.

*Dimethyl 4′-(6-hydroxychromon-3-yl)-2′,6′-dimethyl-1′,4′-dihydropyridine-3′,5′-dicarboxylate (**12**)* Compound **12** was obtained as yellow solid in 66 % yield; M.P. >300 °C; IR (KBr) ν_{max}: 3363, 3234, 1705, 1655, 1621, 1503, 1472, 1342, 1216, 1115, 1022 and 773 cm^{-1}; ^{1}H NMR (400 MHz, DMSO): δ 2.17 (6H, s), 3.52 (6H, s), 4.80 (1H, s), 7.14 (1H, *dd*, *J* = 8.8 and 2.9 Hz), 7.24 (1H, *d*, *J* = 2.9 Hz), 7.40 (1H, *d*, *J* = 8.8 Hz) and 7.84 (1H, s), 8.91 (1H, s), 9.93 (1H, s); ^{13}C NMR (100.5 MHz, DMSO): δ 18.15, 33.12, 50.61, 98.03, 107.59, 119.47, 122.61, 125.02, 125.04, 146.61, 149.11, 153.96, 154.55, 167.48 and 175.22; HRMS (ESI positive mode): *m/z* 408.1048 [M + Na]$^+$, calculated for [$C_{20}H_{19}NO_7$ + Na]$^+$ 408.1054.

*Diethyl 4′-(6-hydroxychromon-3-yl)-2′,6′-dimethyl-1′,4′-dihydropyridine-3′,5′-dicarboxylate (**13**)* Compound **13** was obtained as yellow solid in 64 % yield; M.P. 281–284 °C; IR (KBr) ν_{max} 3308, 3241, 1703, 1657, 1636, 1622, 1471, 1333, 1218, 1116, 1094 and 748 cm^{-1}, ^{1}H NMR (400 MHz, DMSO): δ 1.10 (6H, *t*, *J* = 6.4 Hz), 2.17 (6H, s) 3.92–4.01 (4H, m), 4.78 (1H, s), 7.14 (1H, *dd*, *J* = 8.7 and 2.8 Hz), 7.25 (1H, *d*, *J* = 2.8 Hz), 7.42–7.45 (1H, m), 7.86 (1H, s), 8.30 (1H, s) and 8.84 (1H, s); ^{13}C NMR (100.5 MHz, DMSO): δ 14.07, 18.41, 33.18, 58.96, 98.23, 107.66, 119.40, 121.44, 122.46, 126.54, 146.32, 154.26, 154.53, 156.90, 167.09 and 174.91; HR-ESI-TOF-MS: *m/z* 436.1343 [M + Na]$^+$, calculated for [$C_{22}H_{23}NO_7$ + Na]$^+$ 436.1367.

*Diethyl 4′-(7-acetoxychromon-3-yl)-2′,6′-dimethyl-1′,4′-dihydropyridine-3′,5′-dicarboxylate (**14**)* Compound **14** was obtained as yellow solid in 78 % yield; M.P. 197–199 °C; IR (KBr) ν_{max} 3340, 1767, 1702, 1666, 1634, 1493, 1367, 1204, 1183, 1020, 912 and 745 cm^{-1}, ^{1}H NMR (400 MHz, $CDCl_3$): δ 1.25 (6H, *t*, *J* = 7.3 Hz), 2.28 (6H, s), 2.34 (3H, s), 4.06–4.15 (4H, m), 4.86 (1H, s), 7.10 (1H, *dd*, *J* = 8.8 and 2.2 Hz), 7.24 (1H, *d*, *J* = 2.2 Hz), 7.89 (1H, s), 8.00 (1H, s) and 8.13 (1H, *d*, *J* = 8.8 Hz); ^{13}C NMR (100.5 MHz, $CDCl_3$): δ 14.34, 19.49, 21.10, 35.49, 59.49, 97.94, 110.94, 119.13, 122.94, 125.35, 126.73, 147.37, 153.95, 155.05, 156.36, 167.72, 168.60 and 176.34; HR-ESI-TOF-MS: *m/z* 478.1465 [M + Na]$^+$, calculated for [$C_{24}H_{25}NO_8$ + Na]$^+$ 478.1472.

*Diethyl 4′-(7-hexanoyloxychromon-3-yl)-2′,6′-dimethyl-1′,4′-dihydropyridine-3′,5′-dicarboxylate (**15**)* Compound **15** was obtained as yellow solid in 70 % yield; M.P. 193–195 °C; IR (KBr) ν_{max} 3311, 2961, 1764, 1698, 1663, 1632, 1495, 1309, 1213, 1179, 1123, 1093, 846 and 777 cm^{-1}, ^{1}H NMR (400 MHz, $CDCl_3$): δ 0.94 (3H, *t*, *J* = 7.0 Hz), 1.25 (6H, *t*, *J* = 7.3 Hz), 1.37–1.42 (4H, m), 1.75–1.79 (2H, m), 2.29 (6H, s), 2.59 (2H, *t*, *J* = 7.2 Hz), 4.07–4.13 (4H, m), 4.86 (1H, s), 7.08 (1H, *dd*, *J* = 8.8 and 2.2 Hz), 7.22 (1H, *d*, *J* = 2.2 Hz), 7.44 (1H, s), 7.99 (1H, s) and 8.14 (1H, *d*, *J* = 8.8 Hz); ^{13}C NMR (100.5 MHz, $CDCl_3$): δ 13.87, 14.35, 19.61, 22.26, 24.44, 31.18, 34.29, 35.39, 59.44, 98.22, 110.89, 119.14, 122.88, 125.38 and 126.79, 147.05, 154.11, 154.98 and 156.38, 167.69, 171.51 and 176.32; HR-ESI-TOF-MS: *m/z* 534.2079 [M + Na]$^+$, calculated for [$C_{28}H_{33}NO_8$ + Na]$^+$ 534.2098.

*Dimethyl 4′-(7-acetoxychromon-3-yl)-2′,6′-dimethyl-1′,4′-dihydropyridine-3′,5′-dicarboxylate (**16**)* Compound **16** was obtained as yellow solid in 80 % yield; M.P. 236–238 °C; IR (KBr) ν_{max} 3333, 1776, 1679, 1636, 1614, 1442, 1337, 1222, 1182, 1017, 849 and 778 cm^{-1}, ^{1}H NMR (400 MHz, $CDCl_3$): δ 2.29 (6H, s), 2.34 (3H, s), 3.66 (6H, s), 4.87 (1H, s), 7.09 (1H, *dd*, *J* = 8.8 and 2.2 Hz), 7.22 (1H, *d*, *J* = 2.2 Hz), 7.40 (1H, s), 7.98 (1H, s) and 8.14 (1H, *dd*, *J* = 8.8 and 2.2 Hz); ^{13}C NMR (100.5 MHz, $CDCl_3$): δ 19.37, 21.08, 35.31, 50.81, 97.91, 110.94,

119.16, 122.86, 125.44 and 126.72, 147.53, 154.00, 154.87 156.36, 168.14, 168.57 and 176.40; HR-ESI-TOF-MS: *m/z* 450.1142 [M + Na]$^+$, calculated for [$C_{22}H_{21}NO_8$ + Na]$^+$ 450.1159.

*Dimethyl 4′-(7-hexanoyloxychromon-3-yl)-2′,6′-dimethyl-1′,4′-dihydropyridine-3′,5′-dicarboxylate (**17**)* Compound **17** was obtained as yellow solid in 77 % yield; M.P. 181–182 °C; IR (KBr) ν_{max} 3318, 2953, 1763, 1706, 1670, 1636, 1438, 1315, 1217, 1131, 1092, 846 and 778 cm^{-1}, ^{1}H NMR (400 MHz, $CDCl_3$): δ 0.94 (3H, *t*, J = 7.3 Hz), 1.36–1.42 (4H, m), 1.77 (2H, pentet, *J* = 7.3 Hz), 2.29 (6H, s), 2.58 (2H, *t*, *J* = 7.7 Hz), 3.66 (6H, s), 4.86 (1H, s), 7.08 (1H, *dd*, *J* = 8.8 and 2.2 Hz), 7.22 (1H, *d*, *J* = 2.2 Hz), 7.39 (1H, s), 7.98 (1H, s) and 8.13 (1H, *d*, *J* = 8.8 Hz); ^{13}C NMR (100.5 MHz, $CDCl_3$): δ 13.84, 19.36, 22.23, 24.39, 31.15, 34.27, 35.32, 50.86, 97.91, 110.90, 119.21, 122.79,125.42, 126.80, 147.55, 154.17, 154.86, 156.39, 168.16, 171.47 and 176.44; HR-ESI-TOF-MS: *m/z* 506.1763 [M + Na]$^+$, calculated for [$C_{26}H_{29}NO_8$ + Na]$^+$ 506.1785.

*Diethyl 4′-(7-acetoxychromon-3-yl)-2′,6′-dipropyl-1′,4′-dihydropyridine-3′,5′-dicarboxylate (**18**)* Compound **18** was obtained as yellow solid in 85 % yield; M.P. 189–191 °C; IR (KBr) ν_{max} 3330, 2968, 1764, 1700, 1668, 1637, 1500, 1441, 1201, 1177, 1091, 907 and 770 cm^{-1}, ^{1}H NMR (400 MHz, $CDCl_3$): δ 0.95 (6H, *t*, *J* = 7.2 Hz), 1.22 (6H, *t*, *J* = 7.3 Hz), 1.59 (4H, brs), 2.31 (3H, s), 2.40–2.48 (2H, m), 2.78–2.85 (2H, m), 4.02–4.14 (4H, m), 4.89 (1H, s), 6.18 (1H, s), 7.04 (1H, *dd*, *J* = 8.7 and 2.3 Hz), 7.17 (1H, *d*, *J* = 2.3 Hz), 7.87 (1H, s) and 8.14 (1H, *d*, *J* = 8.7 Hz); ^{13}C NMR (100.5 MHz, $CDCl_3$): δ 13.99, 14.27, 21.10, 22.06, 34.75, 35.29, 59.54, 98.25, 110.86, 118.86, 122.99, 125.77, 126.90, 150.85, 153.81, 154.89, 156.32, 167.31, 168.62 and 175.83; HR-ESI-TOF-MS: *m/z* 534.2076 [M + Na]$^+$, calculated for [$C_{28}H_{33}NO_8$ + Na]$^+$ 534.2098.

*Diethyl 4′-(7-hexanoyloxychromon-3-yl)-2′,6′-dipropyl-1′,4′-dihydropyridine-3′,5′-dicarboxylate (**19**)* Compound **19** was obtained as yellow solid in 83 % yield; M.P. 139–141 °C; IR (KBr) ν_{max} 3331, 2966, 1766, 1697, 1667, 1634, 1500, 1442, 1201, 1136, 1052, 846 and 769 cm^{-1}, ^{1}H NMR (400 MHz, $CDCl_3$): δ 0.89–0.97 (9H, m), 1.22 (6H, *t*, *J* = 7.4 Hz), 1.35–1.39 (4H, m), 1.59–1.65 (4H, m), 1.70–1.78 (2H, m) 2.39–2.48 (2H, m), 2.56 (2H, *t*, *J* = 7.3 Hz), 2.78–2.85 (2H, m), 4.02–4.15 (4H, m), 4.89 (1H, s), 6.20 (1H, s), 7.03 (1H, *dd*, *J* = 8.7 and 2.3 Hz), 7.16 (1H, *d*, *J* = 2.3 Hz), 7.87 (1H, s) and 8.14 (1H, *d*, *J* = 8.7 Hz); ^{13}C NMR (100.5 MHz, $CDCl_3$): δ 13.85, 13.99, 14.26, 22.12, 22.24, 24.42, 31.15, 34.26, 34.70, 35.42, 59.49, 98.07, 110.84, 118.91, 122.88, 125.66, 126.73, 151.13, 153.97, 154.96, 156.35, 167.34, 171.51 and 175.91; HR-ESI-TOF-MS: *m/z* 590.2713 [M + Na]$^+$, calculated for [$C_{32}H_{41}NO_8$ + Na]$^+$ 590.2724.

*Diethyl 4′-(6-acetoxychromon-3-yl)-2′,6′-dimethyl-1′,4′-dihydropyridine-3′,5′-dicarboxylate (**20**)* Compound **20** was obtained as yellow solid in 83 % yield; M.P. 145–148 °C; IR (KBr) ν_{max} 3340, 1764, 1676, 1632, 1572, 1476, 1327, 1217, 1126, 1024 and 776 cm^{-1}, ^{1}H NMR (400 MHz, $CDCl_3$): δ 1.24 (6H, *t*, *J* = 7.3 Hz), 2.30 (6H, s), 2.31 (3H, s), 4.05–4.14 (4H, m), 4.86 (1H, s), 6.52 (1H, s), 7.33 (1H, *dd*, *J* = 8.7 and 2.8 Hz), 7.43 (1H, *d*, *J* = 8.7 Hz), 7.82 (1H, *d*, *J* = 2.8 Hz), 7.97 (1H, s); ^{13}C NMR (100.5 MHz, $CDCl_3$): δ 14.47, 19.84, 21.10, 35.38, 59.87, 98.38, 117.26, 119.80, 125.03, 125.86, 127.20, 146.32, 153.47, 154.74, 167.74, 169.30 and 175.90; HR-ESI-TOF-MS: *m/z* 478.1469 [M + Na]$^+$, calculated for [$C_{24}H_{25}NO_8$ + Na]$^+$ 478.1472.

*Diethyl 4′-(6-hexanoyloxychromon-3-yl)-2′,6′-dimethyl-1′,4′-dihydropyridine-3′,5′-dicarboxylate (**21**)* Compound **21** was obtained as yellow solid in 82 % yield; M.P. 141–143 °C; IR (KBr) ν_{max} 3328, 2980, 1724, 1692, 1674, 1625, 1477, 1330, 1210, 1164, 1087, 826 and 776 cm^{-1}, ^{1}H NMR (400 MHz, $CDCl_3$): δ 0.93 (3H, *t*, *J* = 7.2 Hz), 1.24 (6H, *t*, *J* = 7.1 Hz), 1.37–1.39 (4H, m), 1.71–1.77 (2H, m), 2.30 (6H, s), 2.56 (2H, *t*, *J* = 7.2 Hz), 4.05–4.10 (4H, m), 4.86 (1H, s), 6.38 (1H, s), 7.32 (1H, *dd*, *J* = 9.2 and 2.7 Hz), 7.43 (1H, *d*, *J* = 9.2 Hz), 7.81 (1H, *d*, *J* = 2.7 Hz) and 7.97 (1H, s); ^{13}C NMR (100.5 MHz, $CDCl_3$): δ 13.86, 14.42, 19.94, 22.26, 24.69, 31.23, 34.22, 35.34, 59.62, 98.78, 117.54, 119.41, 125.02, 125.86 and 127.26, 146.31, 147.34, 153.50 and 154.90, 167.59, 172.17 and 176.15; HR-ESI-TOF-MS: *m/z* 534.2082 [M + Na]$^+$, calculated for [$C_{28}H_{33}NO_8$ + Na]$^+$ 534.2098.

*Dimethyl 4′-(6-acetoxychromon-3-yl)-2′,6′-dimethyl-1′,4′-dihydropyridine-3′,5′-dicarboxylate (**22**)* Compound **22** was obtained as yellow solid in 85 % yield; M.P. 276–277 °C; IR (KBr) ν_{max} 3331, 1766, 1683, 1634, 1619, 1476, 1330, 1220, 1126, 1024 and 775 cm^{-1}, ^{1}H NMR (400 MHz, $CDCl_3$): δ 2.28 (6H, s), 2.32 (3H, s), 3.65 (6H, s), 4.88 (1H, s), 7.35 (1H, *dd*, *J* = 9.2 and 2.8 Hz), 7.44–7.47 (2H, m), 7.78 (1H, *d*, *J* = 2.8 Hz) and 8.02 (1H, s); ^{13}C NMR (100.5 MHz, $CDCl_3$): δ 19.52, 20.99, 35.22, 50.87, 98.14, 117.33, 119.44, 125.03, 125.71 and 127.24, 147.22, 153.47, 154.85, 168.11, 169.31 and 176.39; HR-ESI-TOF-MS: *m/z* 450.1144 [M + Na]$^+$, calculated for [$C_{22}H_{21}NO_8$ + Na]$^+$ 450.1159.

*Dimethyl 4′-(6-hexanoyloxychromon-3-yl)-2′,6′-dimethyl-1′,4′-dihydropyridine-3′,5′-dicarboxylate (**23**)* Compound **23** was obtained as yellow solid in 85 % yield; M.P. 192–193 °C; IR (KBr) ν_{max} 3333, 2953, 1759, 1697, 1672, 1621, 1497, 1311, 1225, 1143, 1053, 827 and 771 cm^{-1}, ^{1}H NMR (400 MHz, $CDCl_3$): δ 0.93 (3H, *t*, *J* = 7.8 Hz),

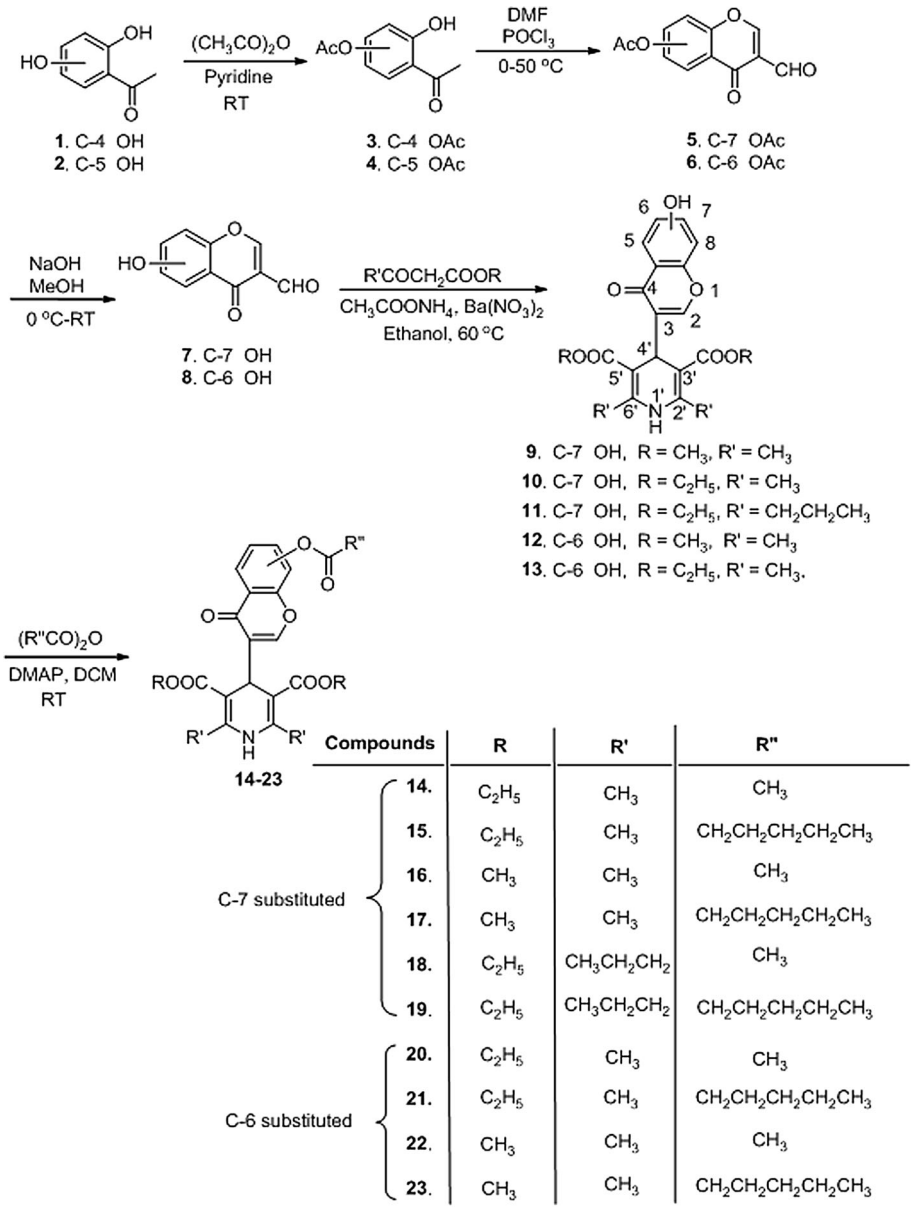

	Compounds	R	R'	R"
C-7 substituted	14.	C_2H_5	CH_3	CH_3
	15.	C_2H_5	CH_3	$CH_2CH_2CH_2CH_2CH_3$
	16.	CH_3	CH_3	CH_3
	17.	CH_3	CH_3	$CH_2CH_2CH_2CH_2CH_3$
	18.	C_2H_5	$CH_3CH_2CH_2$	CH_3
	19.	C_2H_5	$CH_3CH_2CH_2$	$CH_2CH_2CH_2CH_2CH_3$
C-6 substituted	20.	C_2H_5	CH_3	CH_3
	21.	C_2H_5	CH_3	$CH_2CH_2CH_2CH_2CH_3$
	22.	CH_3	CH_3	CH_3
	23.	CH_3	CH_3	$CH_2CH_2CH_2CH_2CH_3$

Scheme 1 Synthesis of 2,6-dialkyl-4-chromon-3-yl-1,4-dihydropyridine-3,5-dicarboxylates (**14–23**)

1.37–1.40 (4H, m), 1.75 (2H, pentet, $J = 7.8$ Hz), 2.28 (6H, s), 2.56 (2H, *t*, $J = 7.8$ Hz), 3.65 (6H, s), 4.88 (1H, s), 7.33–7.35 (2H, m), 7.44 (1H, *d*, $J = 8.7$ Hz), 7.78 (1H, *d*, $J = 2.7$ Hz) and 8.01 (1H, s); ^{13}C NMR (100.5 MHz, $CDCl_3$): δ 13.86, 19.54, 22.26, 24.54, 31.18, 34.19, 35.19, 50.86, 98.20, 117.34, 119.41, 125.02, 125.72, 127.31, 147.14, 147.32, 153.42, 154.82, 168.09, 172.19 and 176.42; HR-ESI-TOF-MS: *m/z* 506.1767 $[M + Na]^+$, calculated for $[C_{26}H_{29}NO_8 + Na]^+$ 506.1785.

BACE-1 enzyme inhibition assay

All the synthesized compounds **14–23** were assessed for their BACE-1 enzyme inhibitory activity. Enzyme inhibition activities were determined using a Förster resonance energy transfer (FRET) assay with recombinant human BACE-1 and quenched fluorescent peptide substrate on the basis of Swedish mutant APP sequence (SEVNLDAEFK). FRET assay kit was purchased from Life Technologies, and the assay was performed on the basis of the manufacturer instructions using a multimode microplate reader (BMG LABTECH, Polar star, Germany).

For carrying out the assay, the provided BACE-1 (purified baculovirus-expressed) and the peptide substrate (Rh-EVNLDAEFK-Quencher) as well as the stock solutions of inhibitors dissolved in DMSO were diluted in the assay buffer (50 mM sodium acetate, pH 4.5). The final concentration of DMSO was kept below 4 %. BACE-1 and test samples (10 µl of each) were placed in 96-well plates. Then, BACE-1 substrate (10 µl) was added to the mixture

and the plates were incubated at 25 °C for 90 min in the dark. The reaction was stopped with 2.5 M sodium acetate, and fluorescence signals were recorded at 544 nm (excitation) and 590 nm (emission) wavelengths to monitor the hydrolysis of the substrate. OM99-2 (Glu-Val-Asn-Leu-Ψ-Ala-Ala-Glu-Phe, Calbiochem) was used as a reference inhibitor compound.

The percentage of enzyme inhibition for each concentration of test compounds was calculated using the Eq. (1):

$$\% \text{ Enzyme inhibition } = {}^{(E-D)}\Big/_{(E-S)} \times 100 \quad (1)$$

where E is the fluorescence emission of maximum enzyme activity (wells containing substrate plus enzyme), D indicates fluorescence emission for wells containing the test compounds (dihydropyridine plus substrate and enzyme), and S represents the baseline fluorescence emission. Each experiment was repeated three times, and BACE-1 inhibition values were presented as mean ± S.E.

Molecular docking study

Flexible-ligand docking studies were carried out using AutoDock version 4.2 (Morris *et al.*, 2009).

X-ray crystallographic *holo* structures of BACE-1 were all retrieved from the Brookhaven Protein Data Bank (2B8L, 2B8V, 2IS0, 2IRZ, 2QMF, 2VJ9, 2VKM; http://www.rcsb.org/).

The protein structure was subjected to optimization step in order to minimize the crystallographically induced bond clashes using steepest descent method by GROMACS package (Van Der Spoel *et al.*, 2005). For preparation of a target protein as a template, cognate ligand and all crystallographic water molecules were removed from the original receptor structure. All the preprocessing steps for receptor crystallographic file (PDB code 2IRZ) were performed within WHAT IF server (http://swift.cmbi.ru.nl/servers/html/) and AutoDock Tools 1.5.4 program (ADT) (Sanner, 1999; Morris *et al.*, 2009). ADT program was used to merge nonpolar hydrogens into related carbon atoms of the receptor, and Kollman charges were also assigned. For docked ligands, Gasteiger charges were assigned and torsions degrees of freedom were also allocated by ADT program.

Lamarckian genetic algorithm (LGA) was applied to simulate the binding between dihydropyridine and BACE-1 active site. One hundred independent genetic algorithm (GA) runs were considered for each ligand under study. For Lamarckian GA method, 5.0×10^7 maximum number of evaluations, 27,000 maximum generations, a gene mutation rate of 0.02 and a crossover rate of 0.8 were used. A grid of 60 × 60 × 60 points in x, y and z direction was built on the center of BACE-1 catalytic site (spacing 0.375 Å). Cluster analysis was performed on the docked results using a root mean square (RMS) tolerance of 2 Å. Schematic 2D representations of the ligand–receptor interactions were all generated using LIGPLOT (Wallace *et al.*, 1995).

Results and discussion

Chemistry

Synthesis of desired 2,6-dialkyl-4-chromon-3-yl-1,4-dihydropyridine-3,5-dicarboxylate derivatives was conducted following the routes depicted in Scheme 1. The structures of all the synthesized compounds **3–23** were unambiguously established on the basis of their spectral (IR, ^{1}H NMR, ^{13}C NMR and HRMS) data analysis. The structures of known compounds **3–8** were further confirmed by the comparison of their physical and spectral data with those reported in the literature (Nohra *et al.*, 1974; Kumar *et al.*, 2007; Chand *et al.*, 2014).

Determination of BACE-1 inhibition

BACE-1 enzyme inhibitory activities of synthesized 1,4-dihydropyridines were determined using a FRET-based kit. Activities were measured as the percentages of enzyme inhibition at the concentrations of 10 and 50 μM of test compounds (Table 1).

The main focus of this study was to find out novel dihydropyridine-based BACE-1 inhibitors with the aim of finding important structural prerequisites for an optimal BACE-1 inhibitory activity. Enzyme inhibitions at 10 μM were used for comparing the potencies of test compounds.

Table 1 In vitro BACE-1 enzyme inhibitory activities of synthesized 1,4-dihydropyridine compounds

Compound	Inhibition at 50 μM (%)[a]	Inhibition at 10 μM (%)
14	37.27 ± 2.64	51.32 ± 0.60
15	9.05 ± 3.56	15.15 ± 4.51
16	39.30 ± 2.63	36.74 ± 2.99
17	3.10 ± 6.39	19.09 ± 1.31
18	23.78 ± 3.95	32.15 ± 5.26
19	12.65 ± 3.36	41.40 ± 4.09
20	32.54 ± 2.78	22.91 ± 2.00
21	3.03 ± 0.93	12.24 ± 3.27
22	44.10 ± 1.80	34.79 ± 8.29
23	37.58 ± 3.14	6.84 ± 3.82

[a] Values represent mean ± standard error (SE) of three independent experiments. IC_{50} value for OM99-2 determined as the reference BACE-1 inhibitor was 0.003 ± 0.001 μM

Table 2 Docking validation results for different *holo* PDB structures of BACE-1 using AutoDock 4.2

PDB code	Structure of cognate ligand	Resolution (Å)	GGA runs	Maximum number of energy evaluations	Population in the optimum cluster (%)	RMSD from reference structure (Å)
2B8L	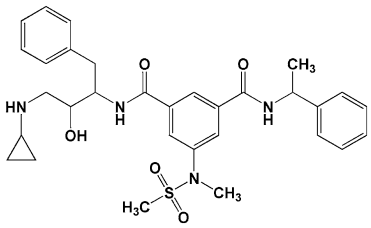	1.70	100	5.0×10^6	47	0.515
2B8V	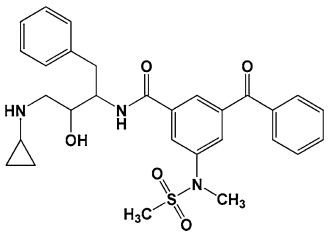	1.80	100	5.0×10^6	80	0.533
2IRZ	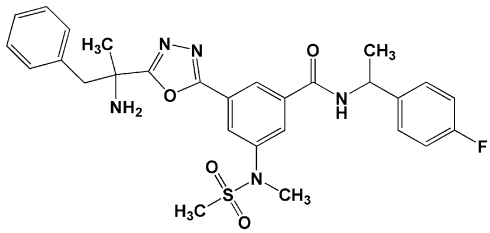	1.80	100	5.0×10^6	88	0.478
2IS0	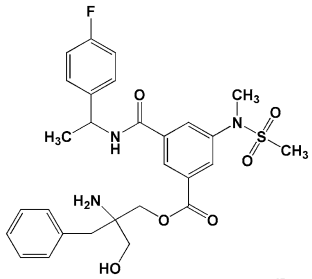	2.20	100	5.0×10^6	27	0.414
2QMF	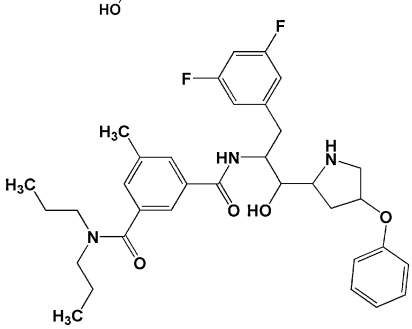	1.75	100	5.0×10^6	18	1.157

Table 2 continued

PDB code	Structure of cognate ligand	Resolution (Å)	GGA runs	Maximum number of energy evaluations	Population in the optimum cluster (%)	RMSD from reference structure (Å)
2VJ9	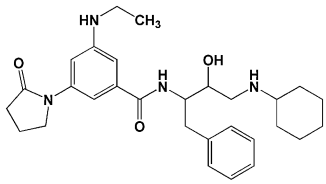	1.60	100	5.0×10^6	34	0.479
2VKM	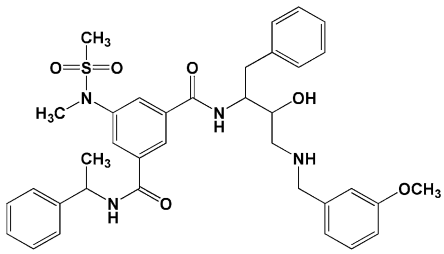	2.05	100	5.0×10^6	25	1.616

Assessment of the structure activity relationship of synthesized derivatives resulted in the following observations:

1. Some of the dihydropyridine derivatives exhibited higher BACE-1 inhibitory activity at 10 μM compared with the activity exhibited at 50 μM. The wells containing the 50 μM concentration of these compounds had generally very high fluorescence emissions from the beginning of incubation time (data not shown), and it was assumed that these compounds had an interference with the FRET assay at higher concentrations. However, low aqueous solubility at higher amounts due to the lipophilic structure of these dihydropyridine compounds could have also contributed to this issue.
2. Compounds **14**, **16**, **18**, **19** and **22** were the most active agents, and all of them exhibited >30 % enzyme inhibition at 10 μM.
3. The presence of the 4-[7-(ethanoyloxy)-4-oxo-4H-chromen-3-yl] moiety at C4 of the dihydropyridine ring (**14**, **16** and **18**) seemed to confer higher activity in comparison with 4-[6-(ethanoyloxy)-4-oxo-4H-chromen-3-yl] (**20** and **22**), 4-[7-(hexanoyloxy)-4-oxo-4H-chromen-3-yl] (**15**, **17** and **19**) and 4-[6-(hexanoyloxy)-4-oxo-4H-chromen-3-yl] (**21** and **23**) substituents at this position.
4. Inappropriate orientation of bulkier 4-[7-(hexanoyloxy)-4-oxo-4H-chromen-3-yl] and 4-[6-(hexanoyloxy)-4-oxo-4H-chromen-3-yl] groups in the active site of BACE-1 may partly explain the observed order. An exception to this notion was compound **19**, which in spite of bearing the 4-[7-(hexanoyloxy)-4-oxo-4H-chromen-3-yl] group at the C4 formation of the dihydropyridine ring, exhibited the second top BACE-1 inhibitory activity.
5. Compound **19** was the only agent bearing *n*-propyl substituents at the C2 and C6 positions of dihydropyridine ring. This could provide additional lipophilic contacts with the active site and probably explain its higher activity.
6. Among the compounds bearing 4-[7-(ethanoyloxy)-4-oxo-4H-chromen-3-yl] moiety at C4 of the dihydropyridine ring (**14**, **16** and **18**), compound **14** with ethoxycarbonyl at C3/C5 and methyl moieties at C2/C6 was the most active compound. This rule seemed to be quite different among compounds bearing 4-[6-(ethanoyloxy)-4-oxo-4H-chromen-3-yl] at C4, in which the presence of methoxy carbonyl at C3/C5 rendered the compound **22** more active than the compound **20**.

Molecular docking

The 3D structures of protein targets are valuable sources of information in modern drug discovery. In this regard, available X-ray crystallographic data from the protein data bank have facilitated the performance of docking simulation studies. In docking, stereoelectronic fit of ligand and its receptor is modeled (Putta and Beroza, 2007). AutoDock is a qualified docking program that has facilitated the process of drug design (The AutoDock Web site. http://autodock.scripps.edu) (Sellers *et al.*, 2010).

Table 3 AutoDock-based binding affinities and lipophilicity indices for 2,6-dialkyl-4-aryl-1,4-dihydropyridine-3,5-dicarboxylates in the active site of BACE-1

Compound code	Estimated Ki (nM)	Estimated pKi	ClogP
14	46.33	4.334	3.21
15	83.93	4.076	4.80
16	101.20	3.995	2.58
17	152.92	3.816	4.10
18	48.93	4.310	4.85
19	30.76	4.512	6.10
20	83.33	4.079	3.19
21	130.45	3.885	4.77
22	75.57	4.122	2.57
23	188.83	3.724	4.02

With the aim of achieving possible ligand–receptor binding features, we focused on molecular docking of synthesized dihydropyridine derivatives on the active site of BACE-1 as a protein target for treatment of AC. For this purpose, docking validation step was performed by re-docking of the co-crystallized conformation of cognate ligands into 3D structures of BACE-1. PDB structures were chosen on the basis of crystallographic resolutions and also relative similarity of co-crystallized ligands to the dihydropyridine structures (http://www.rcsb.org/).

In this way, applied AutoDock 4 program could be tested for predictability of known binding poses (RMSD $\leq$ 2 Å) (Cosconati *et al.*, 2010). Following this rationale, BACE-1 structure with the PDB code of 2IRZ (Rajapakse *et al.*, 2006) was selected for our further

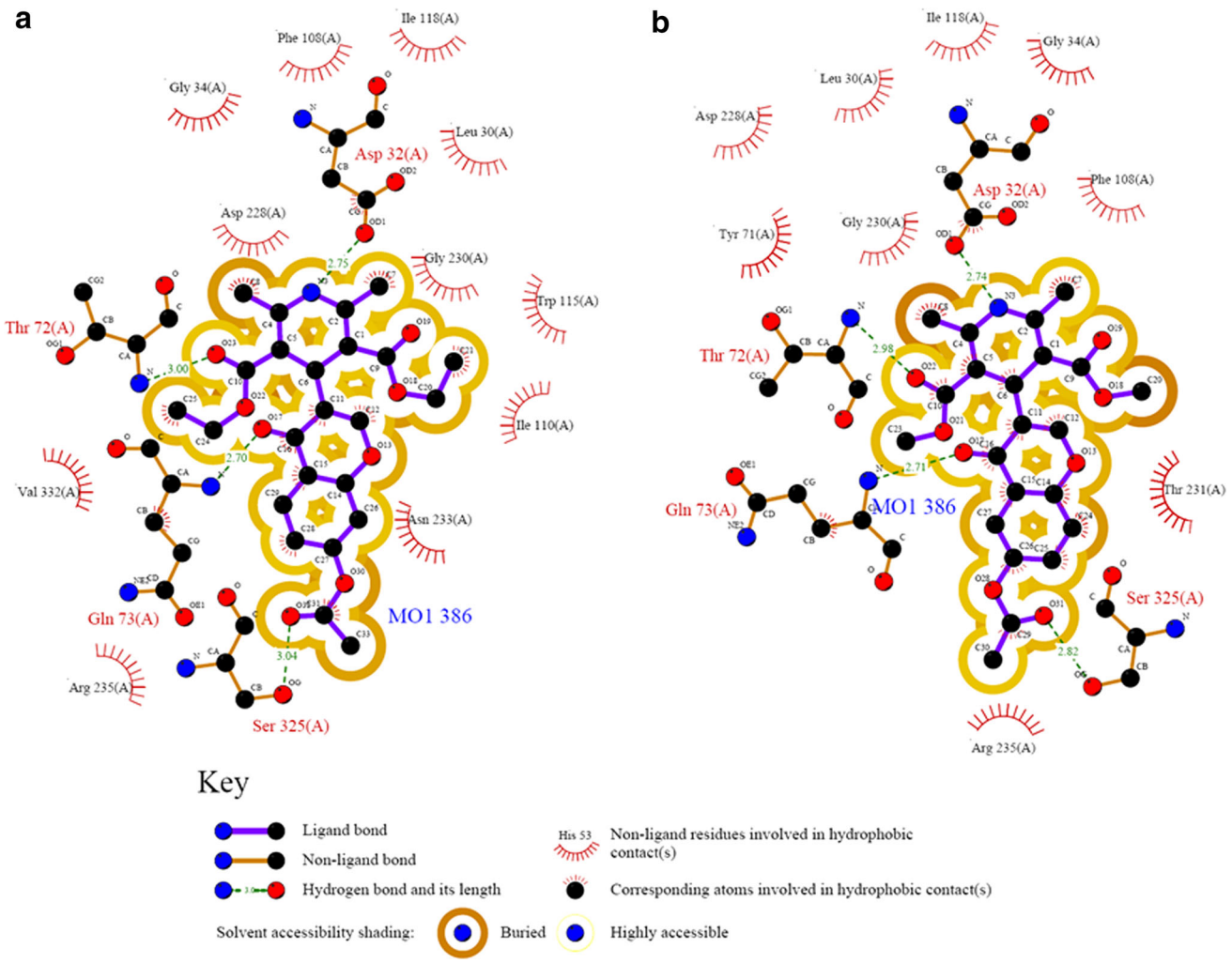

Fig. 1 2D schematic representations of the interactions of the most potent synthetic compounds, **14** (**a**) and **22** (**b**) with the active site of BACE-1

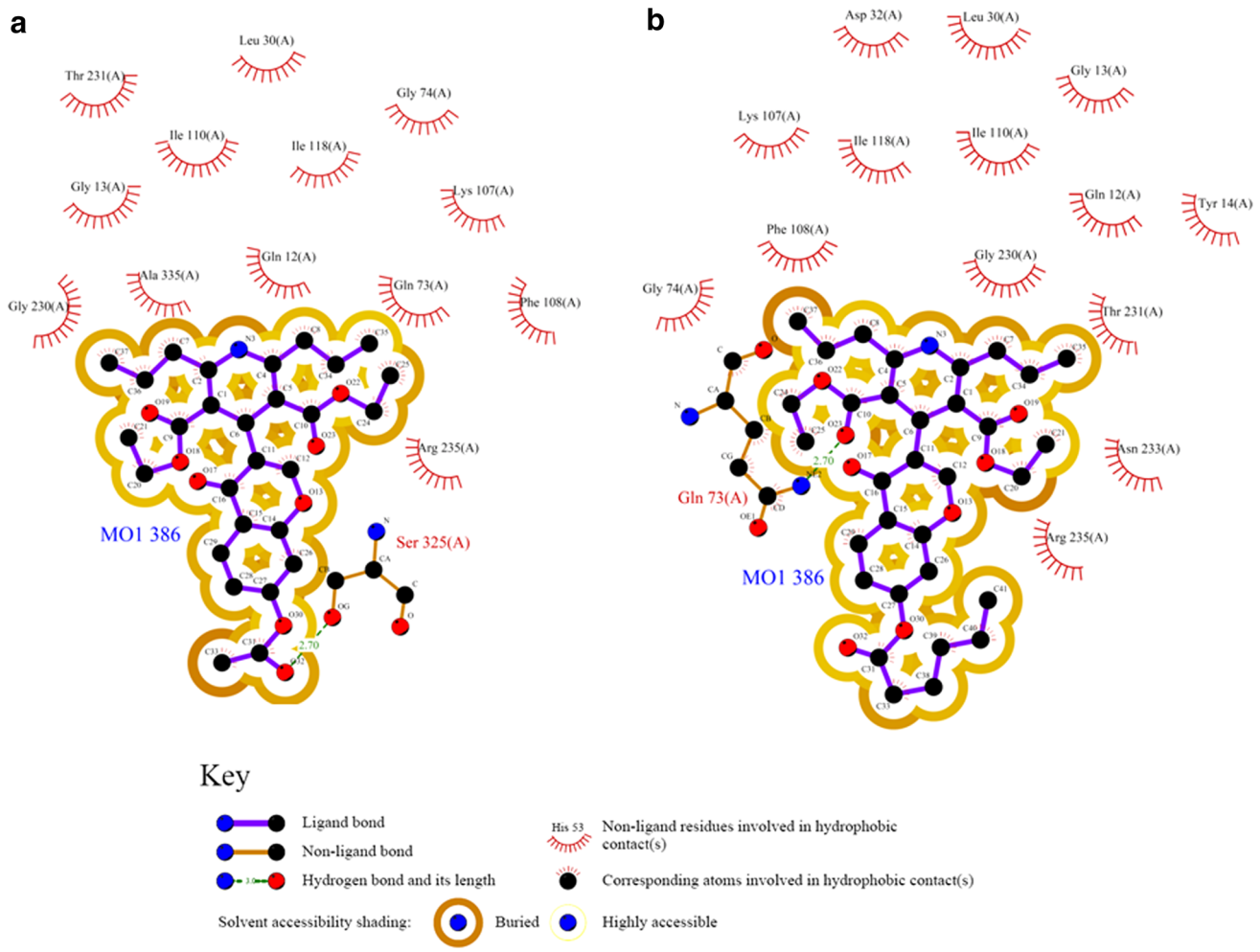

Fig. 2 2D schematic representations of the interactions of compounds **18** (**a**) and **19** (**b**) with the active site of BACE-1

docking simulations. Results of docking validation step are summarized in Table 2.

Our docking procedure provided some insight into the ligand–enzyme binding poses. Estimated free binding energies for dihydropyridine molecules are summarized in Table 3. All the lipid/aqueous partition coefficients were also estimated using online ALOGPS 2.1 program (Tetko *et al.*, 2001; Tetko and Tanchuk, 2002).

Following structure-binding relationships could be developed regarding the obtained in silico results:

1. In almost all docked dihydropyridine structures, a key hydrogen bond between dihydropyridine's NH and Asp32 carboxylate oxygen supported a possible interaction with one of the catalytic dyad residues.
2. LIGPLOT diagrams showed that another participant of BACE-1 catalytic dyad (Asp228) interacted with dihydropyridine structures through hydrophobic contacts.
3. H-bond interaction with S1 subpocket of BACE-1 was detected between the carbonyl oxygen of the ester group and Thr72. Another important H-bond might be expected between carbonyl moiety of chromenon and Gln73. As can be seen in Fig. 1, major lipophilic interactions with the active site of BACE-1 might be observed within S1 and S2 subpockets.
4. The exceptions to the above observation were compounds **18** and **19** in which the presence of *n*-propyl groups at C2 and C6 positions of dihydropyridine ring might distort the molecule and hence avoid additional lipophilic contacts with BACE-1 active site.
5. Different H-bond patterns were observed for compounds **18** and **19**. Compound **18** made H-bond with Ser325 side chain via its 4-[7-(ethanoyloxy)-4-oxo-4H-chromen-3-yl] group, while compound **19** participated in hydrogen bonding to the side chain of Gln73 through carbonyl oxygen of the ester group (Fig. 2).
6. All of the compounds bearing hexanoyloxy-4-oxo-4H-chromen-3-yl group at C4 of the dihydropyridine ring might participate in H-bond interaction with the NH

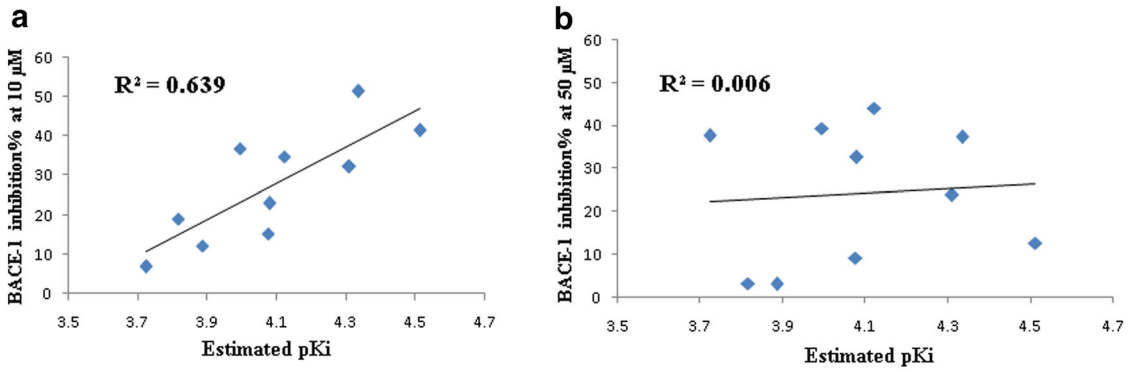

Fig. 3 Correlation of estimated BACE-1 binding affinities (pKi) with in vitro BACE-1 inhibition percentages at 10 µM (**a**) and 50 µM (**b**) concentrations of synthesized 2,6-dialkyl-4-chromon-3-yl-1,4-dihydropyridine-3,5-dicarboxylates

moiety of Asn233 backbone through their hexanoyloxy carbonyl oxygen. The inappropriate orientation of 4-[7-(hexanoyloxy)-4-oxo-4H-chromen-3-yl] and 4-[6-(hexanoyloxy)-4-oxo-4H-chromen-3-yl] groups in the active site of BACE-1 may partly explain the lower inhibitory activities of **15**, **17**, **21** and **23**.

7. Further inspection of the binding maps showed that these four compounds may not form H-bonds with Gln73 and Ser325 unlike the compounds bearing 4-[7-(ethanoyloxy)-4-oxo-4H-chromen-3-yl] (**14** and **16**) or 4-[6-(ethanoyloxy)-4-oxo-4H-chromen-3-yl] substituents (**20** and **22**).

Finally, we found that docking affinities (pK_i) of 2,6-dialkyl-4-aryl-1,4-dihydropyridine-3,5-dicarboxylates could be used to predict the experimental BACE-1 inhibition data at 10 µM ($R^2 = 0.639$; Fig. 3a). Compounds **14** and **19** which were the most potent compounds in enzyme inhibition assay showed also the highest pK_i in the docking study. However, a decent correlation was not observed between pK_i and the inhibition data at 50 µM (Fig. 3b), possibly due to the reasons mentioned earlier in enzyme inhibition section.

Conclusion

Ten 2,6-dialkyl-4-chromon-3-yl-1,4-dihydropyridine-3,5-dicarboxylates were synthesized and evaluated for their in vitro BACE-1 inhibitory activity. Tested dihydropyridine structures were weak-to-relatively-good BACE-1 inhibitors with 6.84 ± 6.62 to 51.32 ± 1.04 percent enzyme inhibitions at 10 µM. SAR exploration of synthesized BACE-1 inhibitors showed that the presence of 4-[7-(ethanoyloxy)-4-oxo-4H-chromen-3-yl] moiety at C4 of the dihydropyridine ring (**14**, **16** and **18**) seemed to generally confer a higher activity compared with other substitutions at this position. Aside from this general notion, compound **19** with 4-[7-(hexanoyloxy)-4-oxo-4H-chromen-3-yl] group at C4 of the dihydropyridine ring was also a potent agent. The presence of *n*-propyl substituents at C2 and C6 of dihydropyridine ring in compound **19**, which is expected to provide additional lipophilic contacts with the BACE-1 active site, could probably explain its higher activity. On the basis of docking simulation studies, a binding pose indicating a key H-bond interaction between Asp32 residue and dihydropyridine NH might be expected in the active site of BACE-1. Moreover, all docked dihydropyridine structures made possibly good hydrophobic contacts with some of the residues of S1 and S2 subpockets. The results of the present study could guide toward rational design of more potent BACE-1 blocking agents on the basis of 2,6-dialkyl-4-(7-(alkyloyloxy)-4-oxo-4H-chromen-3-yl)-1,4-dihydropyridine-3,5-dicarboxylate scaffold.

Acknowledgments The authors wish to thank the Vice-Provost for Research of the Shiraz University of Medical Sciences for the financial support to this project (Grant Number: 93-01-12-8102).

References

Bassil N, Grossberg GT (2009) Novel regimens and delivery systems in the pharmacological treatment of Alzheimer's disease. CNS Drugs 23(4):293–307

Chand K, Prasad S, Tiwari RK, Shirazi AN, Kumar S, Parang K, Sharma SK (2014) Synthesis and evaluation of c-Src kinase inhibitory activity of pyridin-2(1H)-one derivatives. Bioorganic Chem 53:75–82

Chhillar AK, Arya P, Mukherjee C et al (2006) Microwave-assisted synthesis of antimicrobial dihydropyridines and tetrahydropyrimidin-2-ones: novel compounds against aspergillosis. Bioorganic Med Chem 14(4):973–981

Chhillar AK, Yadav V, Kumar A, Kumar M, Parmar VS, Prasad A, Sharma GL (2009) Differential expression of Aspergillus fumigatus protein in response to treatment with a novel antifungal compound, diethyl 4-(4-methoxyphenyl)-2,6-dimethyl-1,4-dihydropyridin-3,5 dicarboxylate. Mycoses 52(3):223–227

Choi SJ, Cho JH, Im I et al (2010) Design and synthesis of 1, 4-dihydropyridine derivatives as BACE-1 inhibitors. Eur J Med Chem 45(6):2578–2590

Cosconati S, Forli S, Perryman AL, Harris R, Goodsell DS, Olson AJ (2010) Virtual screening with AutoDock: theory and practice. Expert Opin Drug Discov 5(6):597–607

Edraki N, Firuzi O, Foroumadi A, Miri R, Madadkar-Sobhani A, Khoshneviszadeh M, Shafiee A (2013) Phenylimino-2H-chromen-3-carboxamide derivatives as novel small molecule inhibitors of β-Secretase (BACE1). Bioorganic Med Chem 21(8):2396–2412

Ghosh AK, Brindisi M, Tang J (2012) Developing β-secretase inhibitors for treatment of Alzheimer's disease. J Neurochem 1:71–83

John V, Beck J, Bienkowski M, Sinha S, Heinrikson R (2003) Human β-secretase (BACE) and BACE inhibitors. J Med Chem 46:4625–4630

Kumar S, Singh BK, Pandey AK, Eycken EVD, Parmar VS, Ghosh B (2007) A chromone analog inhibits TNF-α induced expression of cell adhesion molecules on human endothelial cells via blocking NF-κB activation. Bioorganic Med Chem 15:2957–2962

Kumar RS, Idhayadhulla A, Abdul Nasser AJ, Selvin J (2011) Synthesis and anticoagulant activity of a new series of 1,4-dihydropyridine derivatives. Eur J Med Chem 46(2):804–810

Lahiri DK, Maloney B, Long JM, Greig NH (2014) Lessons from a BACE1 inhibitor trial: off-site but not off base. Alzheimers Dement 10(5 Suppl):S411–S419

McKhann G, Drachman D, Folstein M, Katzman R, Price D, Stadlan EM (1984) Clinical diagnosis of Alzheimer's disease. Neurology 34(7):939–944

Miri R, Javidnia K, Mirkhani H, Kazemi F, Hemmateenejad B, Edraki N, Mehdipour AR (2008) Synthesis and in vitro dual calcium channel antagonist-agonist activity of some 1, 4-dihydo-2, 6-dimethyl-3-nitro and cyano-4-(1-methyl-5-nitro-1H-imidazol-2-yl)-5-pyridinecarboxylates. DARU 16(4):263–270

Miri R, Motamedi R, Rezaei MR, Firuzi O, Javidnia A, Shafiee A (2010) Design, synthesis and evaluation of cytotoxicity of novel chromeno [4,3-b] quinoline derivatives. Arch Pharm 1:111–118

Miri R, Firuzi O, Peymani P, Zamani M, Mehdipour A, Heydari Z, Masteri Farahani M, Shafiee A (2012) Synthesis, cytotoxicity, and QSAR study of new aza-cyclopenta [b] fluorene-1,9-dione derivatives. Chem Biol Drug Des 79(1):68–75

Morris GM, Huey R, Lindstrom W, Sanner MF, Belew RK, Goodsell DS, Olson AJ (2009) AutoDock4 and AutoDockTools4: automated docking with selective receptor flexibility. J Comput Chem 30(16):2785–2791

Nohra A, Umatani T, Sanno Y (1974) Studies on antianaphylactic agents-I: a facile synthesis of 4-oxo-4H-1-benzopyran-3-carboxaldehydes by Vilsmeier reagents. Tetrahedron 30:3553–3561

Putta S, Beroza P (2007) Shapes of things: computer modeling of molecular shape in drug discovery. Curr Top Med Chem 7(15):1514–1524

Rajapakse HA, Nantermet PG, Selnick HG et al (2006) Discovery of oxadiazoyl tertiary carbinamine inhibitors of beta-secretase (BACE-1). J Med Chem 49(25):7270–7273

Razzaghi-Asl N, Firuzi O, Hemmateenejad B, Javidnia K, Edraki N, Miri R (2013) Design and synthesis of novel 3,5-bis-*N*-(aryl/heteroaryl) carbamoyl-4-aryl-1,4-dihydropyridines as small molecule BACE-1 inhibitors. Bioorganic Med Chem 21:6893–6909

Reitz C, Brayne C, Mayeux R (2011) Epidemiology of Alzheimer disease. Nat Rev Neurol 7(3):137–152

Sanner MF (1999) Python: a programming language for software integration and development. J Mol Graph Model 17(1):57–61

Selkoe D (2008) Soluble oligomers of the amyloid β-protein impair synaptic plasticity and behavior. Behav Brain Res 192(1):106–113

Sellers RP, Alexander LD, Johnson VA et al (2010) Design and synthesis of Hsp90 inhibitors: exploring the SAR of Sansalvamide A derivatives. Bioorganic Med Chem Lett 18:6822–6856

Silvestri R (2009) Boom in the development of non-peptidic beta-secretase (BACE1) inhibitors for the treatment of Alzheimer's disease. Med Res Rev 29(2):295–338

Sinha S, Anderson JP, Barbour R, Basi G, Caccavello R, Davis D, Doan M, Dovey H, Frigon N, Hong J (1999) Purification and cloning of amyloid precursor protein β-secretase from human brain. Nature 402(6761):537–540

Tetko IV, Tanchuk VY (2002) Application of associative neural networks for prediction of lipophilicity in ALOGPS 2.1 program. J Chem Inf Comput Sci 42:1136–1145

Tetko IV, Tanchuk VY, Villa AE (2001) Prediction of n-octanol/water partition coefficients from PHYSPROP database using artificial neural networks and E-state indices. J Chem Inf Comput Sci 41:1407–1421

Van Der Spoel D, Lindahl E, Hess B, Groenhof G, Mark AE, Berendsen HJC (2005) GROMACS: fast, flexible, and free. J Comput Chem 26:1701–1718

Vassar R (2002) β-Secretase (BACE) as a drug target for Alzheimer's disease. Adv Drug Deliv Rev 54(12):1589–1602

Verdon CM, Fossati P, Verny M, Dieudonne B, Teillet L, Nadel J (2007) Social cognition: an early impairment in dementia of the Alzheimer type. Alzheimer Dis Assoc Disord 21(1):25–30

Wallace AC, Laskowski RA, Thornton JM (1995) Ligplot-a program to generate schematic diagrams of protein ligand interactions. Protein Eng 8:127–134